Intra-Allelic Suppression of a Mutation that Stabilizes Microtubules and Confers Resistance to Colcemid†

Yaqing Wang,‡ Sudha Veeraraghavan,§ and Fernando Cabral*,‡

Departments of Integrative Biology and Pharmacology, and Biochemistry and Molecular Biology, University of Texas Medical School, 6431 Fannin Street, Houston, Texas 77225

Received February 18, 2004; Revised Manuscript Received May 7, 2004

ABSTRACT: Cmd 4 is a colcemid resistant β-tubulin mutant of Chinese hamster ovary cells that exhibits hypersensitivity to paclitaxel and temperature sensitivity for growth. The mutant β-tubulin allele in this cell line encodes a D45Y amino acid substitution that produces colcemid resistance by making microtubules more stable. By selecting revertants of the temperature sensitive and paclitaxel hypersensitive phenotypes, we have identified three cis-acting suppressors of D45Y. One suppressor, V60A, maps to the same region as the D45Y alteration, and a second suppressor, Q292H, maps to a distant location. Both appear to produce compensatory changes in microtubule assembly that counteract the effects of the original D45Y substitution. Consistent with this view, expression of the V60A mutation in transfected wild-type cells produced paclitaxel resistance and greatly decreased microtubule assembly. Additionally, it produced a paclitaxel-dependent phenotype in which cells grew normally in the presence, but not the absence, of the drug. The Q292H mutation caused even greater disassembly of microtubules such that cells were unable to proliferate when the transgene was expressed; but, unlike the V60A mutation, cell growth could not be rescued by paclitaxel. A third suppressor, A254V, maps to a region near the interface between α- and β-tubulin that contains the colchicine binding site. Although it made transfected wild-type cells hypersensitive to colcemid, it did not affect paclitaxel or vinblastine sensitivity, nor did it reduce microtubule assembly. We suggest that this mutation acts by increasing tubulin's affinity for colcemid.

Microtubules are essential cellular structures responsible for directing vesicle movements, coordinating the orderly segregation of chromosomes prior to cell division, and propelling the movement of ciliated and flagellated cells. Mammalian microtubules are constructed from α- and β-tubulin heterodimers that are products of a multigene family (*1*). In addition to their interest from a biological standpoint, these structures are an important target for a variety of agents used in medicine, most notably in cancer chemotherapy. Because drugs such as vinblastine, vincristine, and paclitaxel have proved to be very effective in the treatment of cancer, much current effort is being directed at developing new drugs, understanding the mechanism by which they affect microtubule assembly, and uncovering the mechanisms by which tumor cells escape their cytotoxicity.

We previously described the isolation of Cmd 4, a Chinese hamster ovary (CHO)[1] cell line resistant to the microtubule inhibitory drug colcemid, and subsequently demonstrated that the cells are temperature sensitive for growth and hypersensitive to paclitaxel (*2*−*4*). More recent studies have shown that Cmd 4 cells produce β-tubulin with a D45Y substitution that stabilizes microtubules. Moreover, a mutation encoding the D45Y substitution was introduced into a cloned β-tubulin cDNA and was shown to be sufficient to confer colcemid resistance when transfected into wild-type CHO cells (*5*). To further explore the role of the D45Y alteration in tubulin structure, microtubule assembly, and drug resistance, we used classical genetic methods to isolate revertants of the temperature sensitive and paclitaxel hypersensitive phenotypes. Here, we describe three intra-allelic alterations that use two distinct mechanisms to suppress the phenotypic effects of the D45Y amino acid substitution.

EXPERIMENTAL PROCEDURES

Growth and Derivation of Cell Lines. Unless otherwise stated, all cell lines were grown in α modification of minimum essential medium (αMEM, Sigma-Aldrich, St. Louis, MO) containing 50 U/mL penicillin, 50 μg/mL streptomycin, and 5% fetal bovine serum (Atlanta Biologicals, Atlanta, GA) at 37 °C and 5% CO_2. Colcemid resistant mutant Cmd 4 was isolated from wild-type CHO cells following mutagenesis with ethyl methanesulfonate (*2*). Spontaneous revertants of Cmd 4 were isolated by selecting cells able to grow at the nonpermissive temperature (40.5 °C) or able to grow in a lethal concentration of paclitaxel (150 ng/mL) as described here and elsewhere (*6*).

Site-Directed Mutagenesis and Transfection. A previously isolated (*6*) CHO β1-tubulin cDNA (GenBank accession no. U08342) was cloned into pTOPneo, a tetracycline regulated

† This work was supported by U.S. Public Health Service Grant CA85935 from the National Cancer Institute (F.C.).

* Corresponding author. Telephone: (713) 500-7485. Fax: (713) 500-7455.

‡ Department of Integrative Biology and Pharmacology.

§ Department of Biochemistry and Molecular Biology.

[1] Abbreviations: CHO, Chinese hamster ovary; Cmd, colcemid; MEM, minimum essential medium; MTB, microtubule stabilizing buffer; PBS, phosphate buffered saline; Ptx, paclitaxel; Tet, tetracycline; Vlb, vinblastine.

10.1021/bi049637b CCC: $27.50
Published on Web 06/25/2004

mammalian expression vector, and transfected into CHO tTApur 6.6a cells that stably express the tetracycline regulated transactivator (*7*). Site-directed mutagenesis of the cDNA was carried out using the Quick Change mutagenesis kit (Stratagene, La Jolla, CA), and transfection was carried out using Lipofectamine (Invitrogen, Carlsbad, CA) as described by the manufacturer except that 1 μg/mL tetracycline was maintained throughout the procedure and subsequent growth of the cells to prevent expression of the transfected cDNA and thereby avoid any potential toxicity from the presence of mutant tubulin gene products. Geneticin (G418, Mediatech Inc., Herndon, VA) was used at 2 mg/mL to select stably transfected cell lines.

Electrophoretic Techniques. Two-dimensional gel electrophoresis was carried out essentially as previously described (*8*, *9*). Cells were labeled for 1 h with 20 μCi/mL Tran ^{35}S-label (mixture of [^{35}S]methionine and [^{35}S]cysteine, 1000 Ci/mmol; ICN Biomedicals, Costa Mesa, CA) in methionine-free MEM (Sigma-Aldrich), lysed in hot (100 °C) SDS sample buffer (*10*), and the proteins were acetone precipitated and redissolved in urea sample buffer (*8*). The 2-D gels were stained with 0.025% Coomassie brilliant blue R250 (Sigma-Aldrich), dried, and exposed to X-Omat film (Eastman Kodak, Rochester, NY). Cellular proteins in SDS were also separated by 1-D gels on 7.5% acrylamide using a minigel apparatus (Bio-Rad, Hercules, CA) and transferred onto nitrocellulose paper (Schleicher and Schuell, Keene, NH) as previously described (*11*). Detection of proteins utilized monoclonal antibodies specific for α-tubulin (DM1A at 1:2000 dilution, Sigma-Aldrich), β-tubulin (Tub 2.1 at 1:2000 dilution, Sigma-Aldrich), or actin (C4 at 1:5000 dilution, Chemicon International Inc., Temecula, CA) followed by peroxidase conjugated goat antimouse IgG (1:2000 dilution, Sigma-Aldrich) and SuperSignal West Pico chemiluminescent substrate (Pierce, Rockford, IL).

Drug Resistance. For each measurement, approximately 200 cells were seeded into each of six replicate wells of a 24-well dish containing growth medium with increasing concentrations of drug and incubated for 7 days until visible colonies appeared. The surviving cells were then stained with 0.5% methylene blue in water, dried, and photographed (*4*). To obtain quantitative data, the dye was eluted into 200 μL of 1% SDS in water, 100 μL was transferred to individual wells of a 96-well dish, and the absorbance was read at 630 nm using an Emax microplate reader (Molecular Dynamics, Sunnyvale, CA). The highest optical density in a series was set at 100%, and the relative values were plotted using pro Fit software (QuantumSoft, Uetikon am See, Switzerland). IC_{50} values were calculated as the concentration of drug that inhibited growth of the cells by 50%.

Immunofluorescence. Cells were grown on sterile glass coverslips for 2 days to approximately 70% confluence, extracted in a microtubule stabilizing buffer (MTB) (20 mM Tris HCl, pH 6.8, 1 mM $MgCl_2$, 2 mM EGTA, 0.5% Nonidet P-40) containing 4 μg/mL paclitaxel (Sigma) for 90 s at 4 °C, and fixed in methanol at −20 °C for at least 10 min. After rehydration in PBS, the cells were incubated in affinity-purified rabbit HA antibody (1:100 dilution, Bethyl Laboratories, Montgomery, TX) for 1 h at 37 °C followed by Alexa 488-conjugated goat anti-rabbit IgG and 1 μg/mL DAPI (both from Molecular Probes, Eugene, OR). The stained coverslips were mounted onto glass slides over a small drop of Gel/Mount (BioMeda Corp., Foster City, CA) and viewed on an Optiphot microscope equipped with a Plan Apochromat 60X, 1.4 numerical aperture oil objective (Nikon Inc., Melville, NY). Images were acquired using a MagnaFire color digital camera (Optronics, Goleta, CA) attached to a Macintosh G4 computer (Apple Computer, Cupertino, CA).

Measurement of Assembled Tubulin. To measure the distribution of tubulin between nonassembled and polymerized pools, cells were grown to near confluence in 24-well dishes, lysed with MTB containing 0.14 M NaCl and 4 μg/mL paclitaxel, transferred to microcentrifuge tubes, and fractionated into soluble and sedimentable proteins at 12 000*g* at 4 °C as previously described (*12*). The tubulin in each fraction was quantified by first adding an equal volume of an *Escherichia coli* extract containing a GST-α-tubulin fusion protein to each fraction, precipitating the proteins with acetone, and redissolving the precipitated proteins with SDS sample buffer (*5*). Following the separation of proteins on 7.5% polyacrylamide gels and transfer onto nitrocellulose, the tubulin in each fraction was detected using a monoclonal antibody to α-tubulin (1:2000 dilution of DM1A, Sigma-Aldrich) and a Cy5-conjugated goat antimouse IgG (1:2000 dilution, Chemicon). Fluorescent images were acquired using a Storm Imager (Molecular Dynamics), and bands were quantified with a Macintosh computer running the public domain NIH Image program (developed at the U.S. National Institutes of Health and available on the Internet at http://rsb.info.nih.gov/nih-image/). The α-tubulin in each fraction was normalized by dividing by the GST-α-tubulin signal, and the percent of tubulin in the polymerized fraction was calculated as the amount of α-tubulin in the pellet divided by the sum of α-tubulin in both pellet and supernatant fractions, all times 100%.

RESULTS

Isolation of Revertants. Mutant Cmd 4 was selected from ethyl methanesulfonate mutagenized CHO cells by single step exposure to a concentration of colcemid that reduced survival of the cells to below 10^{-5} (*2*). Surviving clones were isolated and then screened for increased resistance to drugs unrelated to microtubule assembly to eliminate those cells that might have survived the selection by acquisition of P-glycoprotein mediated multidrug resistance (*13*). The cells were also screened by 2-D gel electrophoresis to identify cell lines with mobility shifts in tubulin. Cmd 4 was thus identified as a colcemid resistant cell line that expressed an altered β-tubulin polypeptide and had normal sensitivity to puromycin, ethidium bromide, and other drugs that do not target microtubule assembly. On the other hand, the cells were cross-resistant to many other drugs such as vinblastine, maytansine, and griseofulvin that destabilize microtubules but were more sensitive to paclitaxel, a drug that promotes the assembly and stability of microtubules (*14*). When the growth of Cmd 4 was compared to wild-type CHO cells at a variety of temperatures, it was found that Cmd 4 grew less well at elevated temperatures (i.e., wild-type cells could efficiently form colonies at 40.5 °C, but Cmd 4 could not).

To determine whether colcemid resistance, paclitaxel hypersensitivity, and temperature sensitivity for growth are all tied to the alteration in β-tubulin, spontaneous revertants

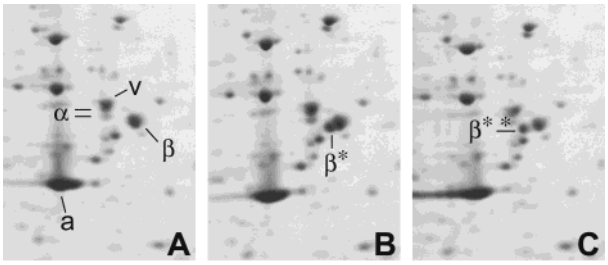

FIGURE 1: 2-D gel electrophoretic analysis of mutant and revertant cell lines. Wild-type (A), Cmd 4 (B), and Tax D3 (C) CHO cells were lysed in SDS sample buffer, and the proteins were precipitated with acetone, resolubilized in urea, and separated by 2-D gel electrophoresis. The basic ends of the gels are to the left. Labeled protein spots include actin (a), vimentin (v), α-tubulin (α), and *β*-tubulin (*β*). Note that α-tubulin migrates as two spots (same isoelectric point, different apparent molecular weights) and that the upper spot partially overlaps vimentin, an intermediate filament protein. All *β*-tubulin proteins in wild-type CHO cells comigrate as a single spot. Cmd 4 (B) has an extra spot (*β**) representing a more basic form of one of the *β*-tubulin gene products, while Tax D3 (C) has a second alteration in the same *β*-tubulin (*β***) that causes the extra spot to migrate to an even more basic position on the gel.

Table 1: Properties of Cmd 4 and Its Revertants

cell line	selection[a]	mutation	Cmd[b]	Ptx[b]	growth (40.5 °C)[c]
wild-type	NA[d]	NA	38.3 ± 5.9	35.2 ± 5.1	+
Cmd 4	Cmd	D45Y	99.9 ± 7.4	24.4 ± 5.4	−
Tax C1	Ptx	D45Y/V60A	32.4 ± 5.4	84.6 ± 6.8	nd
Tax D3	Ptx	D45Y/Q292H	18.9 ± 2.7	104.7 ± 9.3	nd
tR 3H2	40.5 °C	D45Y/A254V	28.4 ± 4.0	25.3 ± 6.7	+

[a] Agent used to select the mutant or revertant cell line. [b] nM IC_{50} values for each drug. [c] Temperature sensitivity (ability to grow at 40.5 °C); −, unable to form colonies; +, able to form colonies; nd, not determined. [d] NA, not applicable.

of the temperature sensitive and paclitaxel hypersensitive phenotypes were isolated. The frequency of spontaneous reversion was surprisingly high, ranging from 8×10^{-5} to 5×10^{-4} for each selection. Most of these revertants had large disruptions of the mutant allele such that no mutant tubulin protein could be detected (Y. Wang and F. Cabral, unpublished), but a few (3/48) continued to produce a stable mutant polypeptide.

The pattern of protein expression in wild-type CHO cells is shown in Figure 1A. Prior studies using antibody labeling, peptide mapping, purification, and transfection demonstrated that all *β*-tubulin proteins in CHO cells migrate as a single spot (*2*, *6*, *15*). Using the nomenclature described by Lopata et al. (*16*), the spot is composed of diploid copies of Class I (70%), Class IVb (25%), and Class V (5%) *β*-tubulin (*15*, *17*). Hereafter, these isoforms will be called *β*1-, *β*4b-, and *β*5-tubulin. Mutant Cmd 4 has an additional spot (*β**) not seen in the wild-type cell extract that migrates with a more basic isoelectric point than wild-type *β*-tubulin (Figure 1B). This spot was previously shown to contain an altered form of one of the two copies of *β*1-tubulin and therefore represented approximately 35% of total *β*-tubulin in Cmd 4 (*6*). Sequence analysis of the gene encoding this altered *β*-tubulin indicated a D45Y substitution that is consistent with the basic shift in the migration of the protein (Table 1). Of the three revertants of Cmd 4 we discuss here, two (Tax C1 and tR 3H2) have 2-D gel patterns identical to Cmd

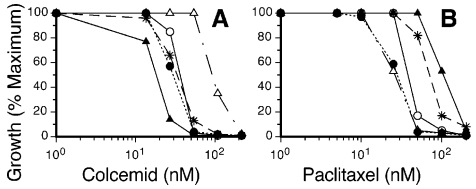

FIGURE 2: Drug sensitivity of mutant and revertant cell lines. Cells were incubated for 7 days in varying concentrations of colcemid (A) or paclitaxel (B), and cell growth was quantified as described in Experimental Procedures. Growth at each concentration of drug was expressed relative to growth without drug set at 100%. Results for wild-type cells (open circles), mutant Cmd 4 (open triangles), and revertants Tax C1 (stars), Tax D3 (solid triangles), and tR 3H2 (solid circles) are shown. Note that, as compared to wild-type cells, Cmd 4 is resistant to colcemid (A) and a little more sensitive to paclitaxel (B). Tax C1 and Tax D3 have lost resistance to colcemid and gained resistance to paclitaxel. tR 3H2, on the other hand, has lost resistance to colcemid but retained increased sensitivity to paclitaxel. Mean IC_{50} values corresponding to each of these curves are summarized in Table 1.

4, but the third (Tax D3) exhibits a further basic shift in the mutant *β**-tubulin, suggesting that the protein now has a second alteration (*β***, Figure 1C). Consistent with these observations, revertants Tax C1 and tR 3H2 were found to have V60A and A254V alterations that would not be expected to alter the mobility of tubulin on 2-D gels, but revertant Tax D3 has a Q292H alteration that can explain the further basic shift in the migration of *β**-tubulin (Table 1).

Revertants Lose Colcemid Resistance. If the D45Y substitution in mutant Cmd 4 is responsible for colcemid resistance, temperature sensitivity for growth, and increased sensitivity to paclitaxel, then revertants selected for loss of temperature sensitivity or paclitaxel hypersensitivity should also lose resistance to colcemid at high frequency. To test this hypothesis, dose responses to colcemid were carried out with each of the three revertants (Figure 2A and Table 1). As predicted, all three revertants lost the colcemid resistance exhibited by the parental mutant Cmd 4, and one of the revertant cell lines, Tax D3, even became colcemid hypersensitive. These results indicate that all three phenotypes (colcemid resistance, temperature sensitivity, and paclitaxel hypersensitivity) arise from changes at a single genetic locus. Moreover, paclitaxel hypersensitivity was lost in Tax C1 and Tax D3 but was retained in tR 3H2 (Figure 2B and Table 1). Loss of paclitaxel hypersensitivity was expected for the first two revertants because that was the basis for their selection. The retention of paclitaxel hypersensitivity in tR 3H2, however, was unexpected based on our previous experience that decreases in colcemid resistance are almost always associated with increases in paclitaxel resistance and vice versa (*18*, *19*). The anomaly in the drug resistance behavior of tR 3H2 was the first clue that the reversion mechanism in this cell line might be unique.

Suppressor Mutations Are in the D45Y Allele. The new mutations uncovered in the revertant strains were found by directly sequencing PCR amplified *β*-tubulin DNA, and so it was not possible to know whether these secondary mutations occurred in the same or a different *β*1-tubulin allele than the one harboring the D45Y mutation. In the case of Tax D3, the 2-D gel analysis strongly argues that the same allele has both mutations because the mutant *β**-tubulin protein undergoes a further basic shift in this cell line. To

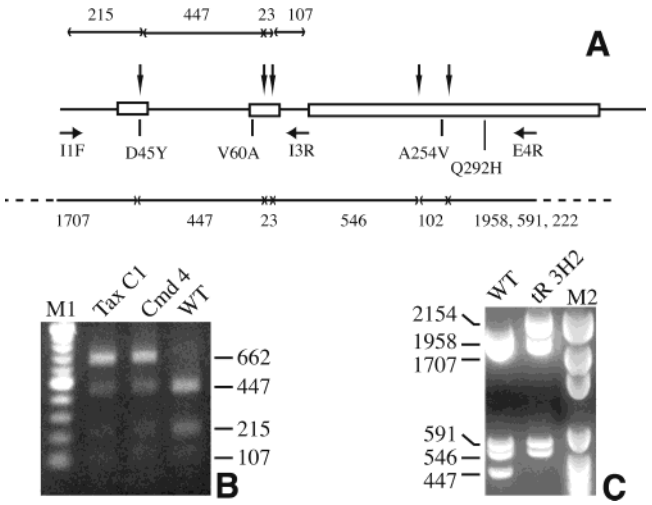

FIGURE 3: *Ava II* digests of wild-type, mutant, and revertant DNA. (A) Diagram of a portion of the β-tubulin gene from intron 1 to the 3′ untranslated region. Positions of mutations and *Ava II* digestion sites (downward facing arrows) are indicated. Above the genomic structure is a PCR amplicon derived using intron 1 forward (I1F) and intron 3 reverse (I3R) primers, with indicated fragment sizes for an *Ava II* digestion of wild-type DNA. Below the genomic structure is a PCR amplicon derived using I1F and exon 4 reverse (E4R) primers cloned into a TOPO TA vector (dotted lines). Predicted fragment sizes for an Ava II digest of wild-type DNA are again indicated. (B) Actual *Ava II* digest of I1F/I3R PCR amplified DNA from the indicated cell lines. Note that Cmd 4 and Tax C1 have a 662 bp fragment due to loss of an Ava II restriction site associated with the D45Y mutation in one of the two β1-tubulin alleles. M1, 100 base pair ladder DNA markers. (C) *Ava II* digests of clones derived from ligating I1F/E4R PCR amplified DNA from tR 3H2 into a TOPO TA cloning vector. Note that the tR 3H2 mutant allele loses a 447 bp fragment that is present in the wild-type allele (WT) but produces a 2154 bp fragment (1707 + 447) because of the loss of the *Ava II* site at D45Y. M2, pGEM DNA Markers (Promega Corp., Madison, WI).

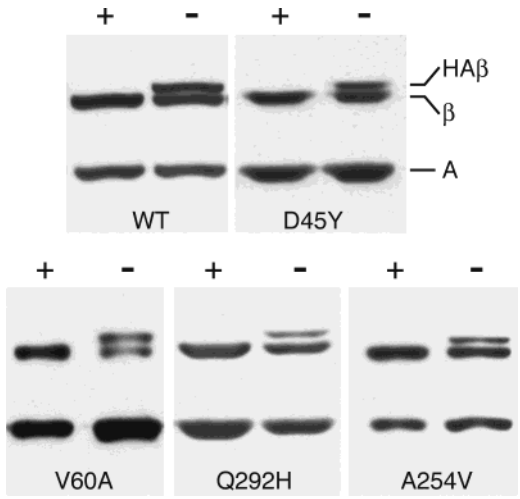

FIGURE 4: Production of mutant tubulin in transfected cells. Cell lines stably transfected with wild-type (WT) HAβ1-tubulin cDNA cloned into a pTOP vector, or with the same DNA modified to encode each of the indicated amino acid substitutions, were grown continuously in αMEM containing 1 μg/mL tetracycline (+) or in the same medium without tetracycline for 2 days (−). The cells were lysed in SDS sample buffer, fractionated by SDS polyacrylamide gel electrophoresis, transferred to nitrocellulose, and probed with mouse monoclonal antibodies Tub 2.1 for β-tubulin (endogenous β and transfected HAβ) and C4 for actin (A). Reactive bands were visualized using chemiluminescence. Note that the figure is a composite from blots run at various times, and the relative intensities of β-tubulin and actin bands may vary because of differences in antibody potencies. The ratio of bands representing HAβ-tubulin to endogenous β-tubulin, however, reflects the relative amount of ectopic β-tubulin production in each of the transfected cell lines.

determine whether V60A is also intra-allelic with D45Y, restriction enzyme digestions of PCR-amplified DNA were carried out. The mutation causing the D45Y substitution changed the wild-type sequence −ctg**g**accga− to −ctg**t**accga− and thereby caused the loss of an *Ava* II restriction site in the mutant DNA. When genomic DNA from the revertant Tax C1 was amplified using primers in introns 1 and 3 and then digested with *Ava* II, the expected digestion pattern (Figure 3A) was obtained. As shown in Figure 3B, control DNA from wild-type CHO cells gave predicted fragments of 447, 215, 107, and 23 bp (lower two bands not clearly seen in the figure), but DNA from mutant Cmd 4 and revertant Tax C1 gave an additional fragment at 662 bp reflecting the loss of the *Ava* II restriction site in the mutant allele. When the 662 base pair band from Tax C1 was excised from the agarose gel and sequenced, it was found to encode both the D45Y and the V60A substitutions, demonstrating that both mutations are in the same allele.

The A254V substitution in revertant tR 3H2 is too distant from D45Y to allow the same approach. In this case, intron 1 forward and exon 4 reverse primers were used for PCR (Figure 3A), and the amplified DNA was ligated to a TOPO TA cloning vector. DNA from random clones was again digested with *Ava* II to identify those containing the D45Y mutation (loss of band at 447, Figure 3C, lane tR 3H2). Sequencing revealed that clones containing the D45Y mutation also contained the A254V mutation, demonstrating that they too are intra-allelic.

Expression of the Suppressor Mutations in a Wild-Type Background. To separate out the effects of the suppressor mutations from those of the D45Y alteration on the phenotypes of the revertant cells, site-directed mutagenesis was used to introduce each suppressor mutation into a pTOP vector that contained a cDNA encoding β1-tubulin with a hemagglutinin (HA) tag at the carboxyl terminus. The pTOP vector was used because its expression in mammalian cells can be repressed by the presence of tetracycline in the culture medium (*7*). This strategy circumvents any potential toxicity resulting from expression of these mutant tubulins. Stably transfected CHO clones were isolated in the presence of tetracycline and then screened for expression of the mutant tubulin when tetracycline was removed. Lysates from cells grown continuously in tetracycline and from cells grown for 2 days without tetracycline were compared by Western blot analysis using an antibody that recognizes all forms of β-tubulin. Clones in which expression of the transgene accounted for 20−50% of total β-tubulin in the cell were chosen for further analysis and are shown in Figure 4. All clones, including cells transfected with a wild-type HAβ1-tubulin cDNA, exhibited little or no expression of the transgene in the presence of tetracycline but produced abundant protein when the antibiotic was removed.

To assess the effects of the mutant tubulins on microtubule organization, immunofluorescence was performed (Figure 5). As we have previously reported (*5*, *12*, *20*, *21*), expression of HAβ1-tubulin had no observable effect on the number or

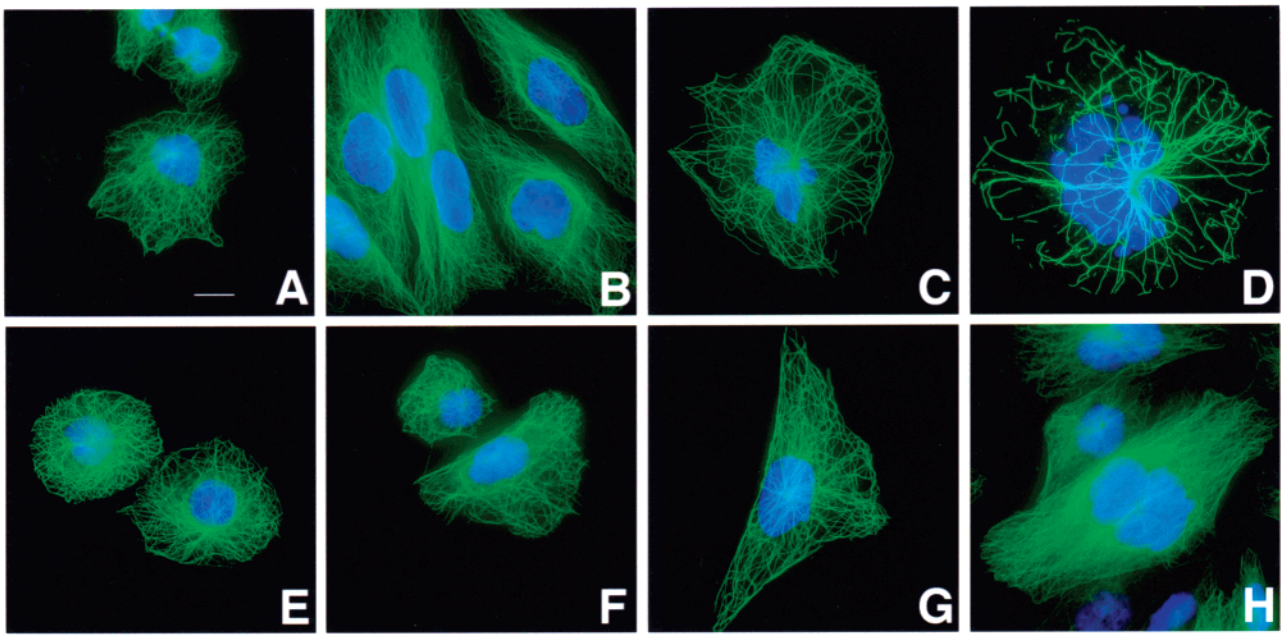

FIGURE 5: Immunofluorescence of cells transfected with wild-type or mutant HAβ1-tubulin cDNA. Cells were grown on glass coverslips, lysed in microtubule stabilizing buffer, fixed in methanol, and reacted with an antibody to the HA tag. Nuclei were stained with DAPI (blue). Cell lines stably transfected with HAβ1-tubulin cDNA containing no mutations (A), D45Y (B), V60A (C), Q292H (D), A254V (E), D45Y/V60A (F), D45Y/Q292H (G), or D45Y/A254V (H) are shown. The bar in panel A is 10 μm.

organization of microtubules (Figure 5A). HAβ1(D45Y)-tubulin expression, on the other hand, produced a denser microtubule network with frequent evidence of microtubule bundling especially in the perinuclear region (Figure 5B). This behavior is consistent with the increased colcemid resistance and increased microtubule assembly previously reported for the Cmd 4 mutant cell line (*12*). Of the three suppressor mutations, A254V (Figure 5E) had little if any effect on microtubules, but V60A (Figure 5C) and Q292H (Figure 5D) caused moderate to dramatic decreases in microtubule density, and in the case of Q292H, produced numerous microtubule fragments. Moreover, DNA staining revealed that cells expressing these latter two mutations accumulated multiple nuclei indicating that the cells had defects in their ability to complete mitosis (*22*). The results suggested that V60A and Q292H reverse the effects of the D45Y mutation by making the microtubules less stable. Consistent with this interpretation, transfection of D45Y/V60A (Figure 5F) and D45Y/Q292H (Figure 5G) double mutants produced microtubule densities closer to those seen with wild-type DNA. In contrast, combining the D45Y and A254V mutations (Figure 5H) produced microtubule density similar to D45Y alone (Figure 5B), arguing that A254V, unlike V60A and Q292H, does not oppose the action of D45Y on microtubule assembly.

Assembled Tubulin Is Reduced in Cells Transfected with V60A and Q292H But Not with A254V. To confirm the visual impression (Figure 5) that cells transfected with cDNAs encoding the V60A and Q292H substitutions have less assembled tubulin, we turned to a biochemical assay that involves lysing cells in a microtubule stabilizing buffer, separating polymerized from soluble tubulin by centrifugation, and quantifying tubulin in each fraction by Western blot analysis (*5*, *12*). The results shown in Figure 6 confirmed the observations from immunofluorescence microscopy. As reported previously, wild-type CHO cells and CHO cells transfected with a wild-type β1-tubulin cDNA encoding a

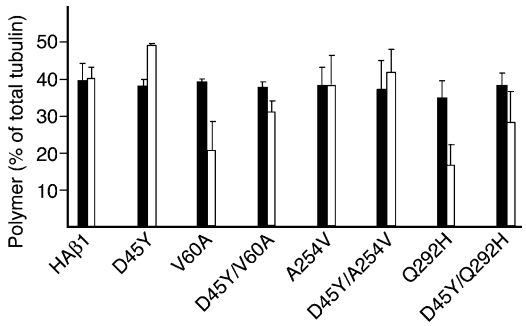

FIGURE 6: Extent of tubulin assembly in transfected cells. Cell lines stably transfected with HAβ1-tubulin or with the same DNA containing each of the indicated mutations were grown in the presence (solid bars) or absence (open bars) of tetracycline and lysed in microtubule stabilizing buffer. Polymerized tubulin was separated from soluble tubulin by centrifugation, and the content of α-tubulin in each fraction was quantified. The extent of assembly is expressed as the percentage of total tubulin (supernatant and pellet) that is present in the pellet fraction alone. The results from cells transfected with DNA containing double mutations (D45/V60A, D45Y/A254V, and D45Y/Q292H) are also shown. At least three separate experiments were run for each cell line, and the error bars represent the standard deviation from the mean.

carboxyl terminal HA epitope tag have approximately 40% of their total cellular tubulin in the polymer fraction (*5*, *7*, *12*, *18*, *20*, *21*) regardless of whether the transgene is expressed (open bars) or not expressed (solid bars). Expression of cDNA encoding the D45Y substitution found in Cmd 4 increased the fraction of polymerized tubulin to approximately 50%, consistent with a mechanism in which incorporation of the altered tubulin stabilizes microtubule assembly. Expression of V60A and Q292H mutations, on the other hand, decreased the fraction of assembled tubulin, supporting the idea that these two mutations reverse the effects of D45Y by destabilizing microtubule assembly. This balancing of stabilizing and destabilizing effects is confirmed by noting that microtubule assembly in cells expressing

Table 2: Drug Resistance of Cells Transfected with Mutant Tubulin cDNAs[a]

	+Tet			−Tet		
cell lines	Ptx	Cmd	Vlb	Ptx	Cmd	Vlb
HAβ1	37.5 ± 8.7	32.7 ± 7.0	9.2 ± 2.3	38.0 ± 3.3	23.5 ± 3.5	7.1 ± 0.5
A254V	35.0 ± 3.3	24.0 ± 3.8	9.8 ± 0.3	33.4 ± 3.0	5.1 ± 1.6	6.8 ± 0.3
D26E	43.1 ± 7.5	41.3 ± 2.7	11.2 ± 0.7	205 ± 17.7	2.2 ± 0.5	2.1 ± 0.2
V60A	40.3 ± 6.8			120 ± 14.1		

[a] IC_{50} values (nM) were determined as described in Experimental Procedures for cell lines stably transfected with HAβ1 cDNA or with the same cDNA mutated to encode A254V, D26E, or V60A amino acid substitutions. Measurements were made on cells grown in the presence (+Tet) and in the absence (−Tet) of tetracycline. Standard deviations were based on two to five experiments. Ptx, paclitaxel; Cmd, colcemid; Vlb, vinblastine.

D45Y/V60A and D45Y/Q292H double mutants was intermediate as compared to either mutation alone. Also in agreement with the immunofluorescence results shown in Figure 5, expression of A254V appeared to have little or no effect on microtubule assembly, again indicating that it reverses the colcemid resistance of D45Y by a different mechanism. Although the level of polymerized tubulin appeared somewhat lower in the D45Y/A254V double mutant than in the D45Y mutant alone, this result was likely due to a lower level of expression in the double mutant (data not shown). Subtle tertiary structural changes induced by the A254V substitution, however, cannot be ruled out as an explanation.

Effects of V60A, A254V, and Q292H Mutations on Drug Resistance. In previous studies, we found that CHO mutants selected for resistance to paclitaxel are frequently hypersensitive to colcemid, and all have alterations in tubulin that make microtubules less stable (*7*, *12*, *18*). Given the ability of the V60A and Q292H suppressor mutations to destabilize microtubule assembly, we predicted that cells expressing these mutant tubulins would exhibit paclitaxel resistance. As demonstrated in Figure 7B and Table 2, this prediction was confirmed for the V60A mutation (stars), which not only produced paclitaxel resistance when expressed but also made the cells paclitaxel dependent (i.e., the cells grew very poorly unless paclitaxel was present in the growth medium). A similar phenotype has previously been described for a subset of mutants selected for paclitaxel resistance using classical genetic methods (*4*, *7*, *23*). A dose−response curve could not be carried out for cells carrying the Q292H mutation because they were unable to proliferate without tetracycline even when paclitaxel was present. This outcome is likely a consequence of the extreme damage inflicted on microtubule assembly when this mutant tubulin is expressed (see Figure 5D) (i.e., the defect produced by assembly of this mutant tubulin was of a kind or extent that could not be corrected even by the presence of a microtubule stabilizing drug). Unlike the Q292H and V60A mutations, expression of the A254V mutation (closed circles) did not produce a change in paclitaxel sensitivity relative to wild-type (Figure 7B).

Because of the growth defects or paclitaxel dependence produced by the Q292H and V60A mutations, sensitivities of cells transfected with these mutant tubulins to colcemid and vinblastine could not be measured. Thus, for comparison of the behavior of the A254V mutation to a typical paclitaxel resistance mutation, we used cells transfected with HAβ1-tubulin containing a D26E substitution (open triangles) that will be described elsewhere (S. Yin and F. Cabral, unpublished). Although cells transfected with this mutant tubulin were a little paclitaxel dependent (Figure 7B), they grew well

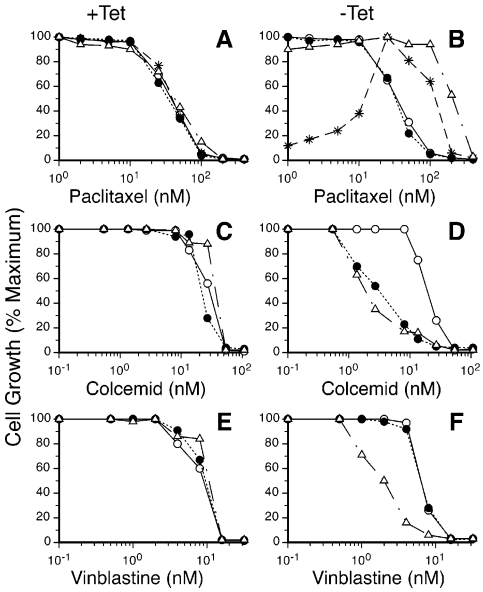

FIGURE 7: Drug resistance of cells stably transfected with HAβ1-tubulin (open circles), or the same cDNA encoding A254V (solid circles), D26E (open triangles), or V60A (stars) substitutions in the presence or absence of tetracycline. Cells were grown for 7 days and then quantified as described in Experimental Procedures. Results are plotted relative to the best conditions for growth for each cell line set at 100%. Note that all cell lines have similar drug sensitivities in the presence of tetracycline (A, C, and E) but differ when the mutant cDNAs are expressed (B, D, and F). Because the growth of cells transfected with HAβ1(V60A) is highly dependent on the presence of paclitaxel (stars, B), another control, HAβ1-(D26E), is included for comparison of sensitivities to colcemid and vinblastine. Mean IC_{50} values corresponding to each of these curves are summarized in Table 2.

enough without paclitaxel to allow sensitivities to colcemid and vinblastine to be measured. Consistent with the microtubule destabilizing effects we have previously reported for paclitaxel resistance mutations, cells expressing the D26E mutation were more sensitive than wild-type to both colcemid (Figure 7D) and vinblastine (Figure 7F). In contrast, the A254V mutation that did not decrease microtubule assembly (Figure 6) increased the sensitivity of transfected cells to colcemid (Figure 7D) but not to vinblastine (Figure 7F).

DISCUSSION

The isolation of revertants has provided new insights into the interplay between microtubule assembly and sensitivity of cells to drugs that interact with tubulin. Previous studies on Cmd 4 indicated that the D45Y alteration in β1-tubulin affected approximately 35% of the total cellular β-tubulin (*6*). Measurements of soluble and polymerized tubulin

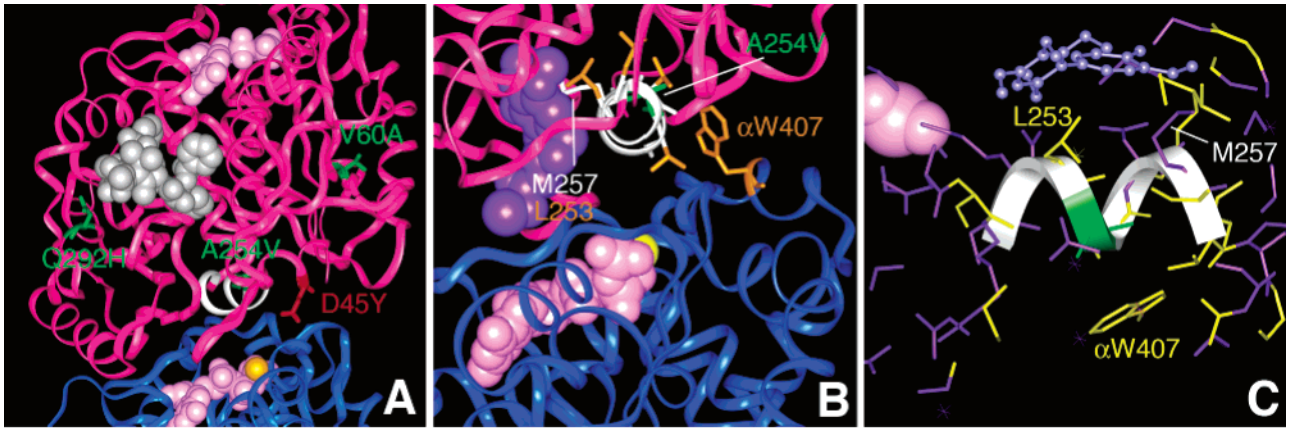

FIGURE 8: Structural model of a tubulin heterodimer. (A) Ribbon diagram based on the coordinates 1JFF (*24*). Tubulin is viewed from the inside of the microtubule. Pink spheres, guanine nucleotides; gray spheres, paclitaxel; yellow sphere, Mg^{2+}; magenta, β-subunit; and blue, α-subunit. Labeled residues include the D45Y colcemid resistance mutation (red) and revertant mutations V60A, Q292H, and A254V (green). Helix 8 (H8) is shown in white and contains the A254V mutation that confers hypersensitivity to colcemid. (B) Closeup of the colchicine binding region based on coordinates 1SA0 (*31*). The orientation represents a 32° clockwise rotation around the *Z*-axis relative to panel A. Lavender spheres represent colchicine. Hydrophobic residues of helix 8 and a proximal W407 from the α subunit are depicted in gold. This view down the H8 axis reveals the largely amphipathic nature of the helix and hydrophobic contacts between residues in H8 and colchicine. The side chains of L253 and M257, which make close contacts with the drug, are indicated. A254 (green) faces away from the drug and toward αW407. (C) Further closeup of the colchicine binding pocket depicting all atoms within 5 Å of H8. The orientation represents −90° (anticlockwise) rotations around the *Z*- and *X*-axes relative to panel B. All nonhydrophobic residues are shown in purple, and hydrophobic residues are shown in yellow. A254 (green) is located in a pocket large enough to accommodate the bulky valine side chain in the A254V mutant. This side view illustrates the large number of hydrophobic contacts to residues in the C-terminal half of helix 8 and close packing of colchicine (shown as ball-and-stick for clarity) including its A and C rings relative to helix 8. The models were drawn and analyzed using Insight II software (Accelrys, San Diego, CA).

showed an increase in the fraction of tubulin that was assembled, consistent with a model in which incorporation of β1-tubulin containing the D45Y substitution stabilized microtubules and led to more assembled tubulin at steady state (*12*). The increased microtubule stability could then explain the increased resistance of Cmd 4 to drugs such as colcemid and vinblastine that destabilize microtubules and the increased sensitivity to drugs such as paclitaxel that stabilize microtubules (*18*, *19*). As further reinforcement of these ideas, we now show that the stabilizing effects of D45Y can be counterbalanced by intra-allelic mutations such as V60A and Q292H that destabilize microtubules, and at least in the case of the V60A mutation, confer paclitaxel resistance when expressed in a wild-type background. Although we anticipated that the Q292H alteration would also confer paclitaxel resistance, its effects on microtubule assembly were more severe as judged by immunofluorescence of microtubules in the transfected cells and by biochemical fractionation studies that indicated very little tubulin in the polymerized fraction. Thus, the structural changes in tubulin produced by the Q292H alteration may produce flaws in the microtubules that cannot be overcome by adding paclitaxel. Interestingly, a Q292E mutation was recently reported in a human lung cancer cell line selected for resistance to epothilone B, another drug that stabilizes microtubules (*23*). We speculate that the ability of this latter mutation to produce epothilone resistance may be due to a less disruptive structural change induced by the glutamic acid versus the histidine substitution at that amino acid position or to the possibility that other changes occurred in the epothilone resistant lung cells during their multistep selection that mitigate the effects of the Q292E mutation.

The positions of the altered amino acids in the tertiary structure of β-tubulin are consistent with the phenotypes they produce. Figure 8A shows a molecular model of tubulin predicted from the published atomic coordinates (PDB 1JFF) (*24*). Aspartic acid 45 (shown in red) is located in a loop connecting helix 1 (H1) with β sheet 2 (S2) of the protein and predicted to be a major contact region between protofilaments forming the wall of the microtubule (*25*). The residue altered in Cmd 4 is thus in a position where it could well increase stability of the microtubule structure. On the other hand, D45Y is not close to the site where colcemid binds to tubulin, making it unlikely to act by changing the affinity of tubulin for the drug. Valine 60, the residue altered in revertant Tax C1, is also in the H1−S2 loop and occupies a position within 15 Å of D45. We demonstrated that an alanine at this position reduces microtubule assembly and confers resistance to paclitaxel. When the D45Y and V60A substitutions are combined, their individual effects on microtubule assembly largely cancel out (Figures 5 and 6), and the sensitivity of transfected cells to paclitaxel and colcemid returns closer to wild-type values (data not shown). It is possible that V60A returns the structure of the H1−S2 loop to a more native conformation or it may weaken a nearby contact point with an adjacent protofilament and in that way counteract the stabilizing effect of the D45Y substitution.

Glutamine 292 is located on the opposite side of β-tubulin from aspartic acid 45 and is in a position to influence the orientation of the M-loop, a region that is also involved in lateral contacts between protofilaments and likely to interact with the H1−S2 loop of tubulin on the adjacent protofilament (*25*). Thus, it appears reasonable to speculate that Q292H reverses the effects of D45Y on microtubule assembly and drug resistance by weakening the same or similar interaction that is strengthened by D45Y.

The locations of the V60A and Q292H alterations near the surface of regions that are predicted to form lateral contacts in the microtubule structure are consistent with their

inhibitory effects on microtubule assembly and with the overall model for the mechanism by which mutations we have characterized in numerous other mutant cell lines confer drug resistance (*18*, *19*, *26*). The nearly invariant observation we have made with these earlier mutants is that mutations that destabilize microtubules confer paclitaxel resistance and colcemid hypersensitivity (*4*), whereas mutations that stabilize microtubules confer colcemid resistance and paclitaxel hypersensitivity (*5*). A254V represents the first departure from this rule we have encountered in analyzing over 50 mutations and is likely to affect drug sensitivity by a distinct mechanism. By itself, A254V does not confer resistance to any drug we have tested but instead confers hypersensitivity to colcemid and its analogue, colchicine. In contrast to other mutations we have studied, A254V has no obvious effect on steady-state microtubule organization or assembly. Also unlike V60A and Q292H, A254V is not located near lateral contact points in assembled microtubules but rather near the intradimer interface (Figure 8A,B), a region that has been implicated in binding colchicine (*27*, *28*). Moreover, A254 is close to M257, a residue that was altered in *Aspergillus nidulans* mutant cells with reduced binding of benomyl, another drug that is likely to bind at or near the colchicine binding site (*29*). Consistent with the hypothesis that A254V affects colcemid binding, we saw no enhanced sensitivity or resistance to vinblastine, a drug that also destabilizes microtubule assembly but binds to a distinct site on tubulin (*30*). This result stands in direct contrast to all other mutations we have examined in drug-resistant CHO cells. In those cells, mutations that confer resistance or hypersensitivity to one drug that inhibits microtubule assembly also confer resistance or hypersensitivity to virtually all other drugs that inhibit microtubule assembly.

These arguments lead us to conclude that A254V probably acts by increasing tubulin's affinity for colcemid. This would explain the ability of the mutant tubulin to increase cell sensitivity to colcemid without affecting the assembly or distribution of microtubules and without abrogating the ability of the D45Y mutation to elevate microtubule assembly and produce microtubule bundling. Our conclusion is further supported by the recent publication of the crystal structure of a tubulin−colchicine complex (PDB 1SA0) (*31*) showing colchicine (lavender spheres) nestled into the β subunit at the intradimer interface (Figure 8B). A254 (green) is located within helix 8 (H8, white, residues 250−257) of β-tubulin, very close to the colchicine binding site. Using this structural model, we considered how the A254V mutation might affect the position, internal stability, or dynamics of H8 to produce increased colchicine sensitivity. In colchicine bound tubulin, H8 (and a turn made of flanking residues) forms one side of the colchicine binding pocket. Side chains of L253 and M257 in H8 make close contacts with the drug, whereas A254 (green) is in the middle of H8 on the outer surface of this pocket, facing away from the drug. When the colchicine-bound (PDB 1SA0) and colchicine-free (PDB 1FXX) structures are superimposed, H8's internal structure, its interactions with other residues in α- and β-tubulin, and its position relative to the dimer interface remain intact (i.e., there is no noticeable conformational change that accompanies drug binding). Moreover, a valine substitution at A254 would be unlikely to disrupt the helical structure of H8, and the A254 pocket itself is large enough to accommodate the valine side chain without distorting the position of H8. Therefore, it is unlikely that the A254V substution acts by causing a significant conformational change around the colchicine binding pocket. What then could lead to increased colchicine sensitivity in the A254V mutant? Examining which atoms fall within a 5 Å radius of H8 reveals that the C-terminal half of the helix has many hydrophobic residues (Figure 8C). Placing a valine instead of an alanine at residue 254 is likely to increase hydrophobic interactions with some of the other hydrophobic residues in H8 and with the proximal αW407 side chain. Such increased hydrophobic contact could lead to greater stabilization of H8's position within the protein or to reduced mobility or dynamics of H8. These localized changes might then preselect a lower energy state for the colchicine pocket that favors colchicine binding. A second possibility is that contacts between colchicine and the H8 residues L253 and M257 are strengthened as a result of the A254V mutation and that in turn could lead to enhanced colchicine affinity.

One might ask why mutations affecting drug binding have been found so rarely in the past. As we have previously argued (*26*), decreased drug binding, such as would be needed to produce drug resistance, is a loss of function recessive phenotype that would be unlikely to be seen in diploid cells that express multiple tubulin genes. Increased drug binding, on the other hand, is a gain of function dominant mutation that can be isolated in such cells. Unfortunately, direct selections for increased drug sensitivity are difficult because the mutant cells are the ones that are dying in the selection. In our case, we were able to isolate the A254V mutation indirectly by selecting for loss of the temperature sensitivity for growth phenotype associated with the D45Y mutation.

The molecular mechanism that allows A254V to reverse the temperature sensitive effects produced by the D45Y mutation is unclear. Previous studies have shown that CHO cells with mutations in α- or β-tubulin and resistant to microtubule stabilizing or destabilizing drugs can exhibit temperature sensitivity for growth (*32*). The fact that temperature sensitivity is not associated with any specific assembly or resistance phenotype tends to argue that the mutations produce temperature sensitivity by making tubulin more susceptible to thermal disruption rather than by altering specific assembly properties or drug binding characteristics. The fact that A254V can reverse both colcemid resistance and temperature sensitivity associated with the D45Y mutation could be fortuitous, or it could suggest some as yet obscure relationship between the colchicine binding region and tubulin thermal stability. In this regard, it is interesting to note that colchicine binding has been reported to stabilize the tubulin heterodimer (*33*). It is tempting to speculate that the A254V alteration could be mimicking some of the structural effects produced by colchicine binding, and this could explain why the binding pocket has increased affinity for the drug. Further studies will be necessary to elucidate the role of the A254V mutation in reversing the temperature sensitive phenotype of Cmd 4, but it is already clear that reversion analysis of drug resistant mutants can provide a useful method to identify interesting mutations that would otherwise be difficult to isolate.

These studies demonstrate that cellular resistance to microtubule inhibitory drugs can revert back to sensitivity

through at least two distinct mechanisms. One mechanism, exemplified by V60A and Q292H mutations, acts by altering microtubule assembly and stability in a manner that opposes the effects of the original D45Y mutation. A second mechanism, exemplified by the A254V mutation, does not oppose the assembly effects of the D45Y mutation and has no direct effect on microtubule assembly and stability on its own. Rather, it appears to act by increasing the affinity of tubulin for the microtubule inhibitory drug.

REFERENCES

1. Sullivan, K. F. (1988) Structure and utilization of tubulin isotypes, *Ann. Rev. Cell Biol. 4*, 687−716.
2. Cabral, F., Sobel, M. E., and Gottesman, M. M. (1980) CHO mutants resistant to colchicine, colcemid, or griseofulvin have an altered β-tubulin, *Cell 20*, 29−36.
3. Cabral, F., Abraham, I., and Gottesman, M. M. (1982) Revertants of a Chinese hamster ovary cell mutant with an altered β-tubulin: evidence that the altered tubulin confers both colcemid resistance and temperature sensitivity on the cell, *Mol. Cell. Biol. 2*, 720−729.
4. Schibler, M., and Cabral, F. (1986) Taxol-dependent mutants of Chinese hamster ovary cells with alterations in α- and β-tubulin, *J. Cell Biol. 102*, 1522−1531.
5. Hari, M., Wang, Y., Veeraraghavan, S., and Cabral, F. (2003) Mutations in α- and β-tubulin that stabilize microtubules and confer resistance to colcemid and vinblastine, *Mol. Cancer Ther. 2*, 597−605.
6. Boggs, B., and Cabral, F. (1987) Mutations affecting assembly and stability of tubulin: evidence for a nonessential β-tubulin in CHO cells, *Mol. Cell. Biol. 7*, 2700−2707.
7. Gonzalez-Garay, M. L., Chang, L., Blade, K., Menick, D. R., and Cabral, F. (1999) β-tubulin leucine cluster involved in microtubule assembly and paclitaxel resistance, *J. Biol. Chem. 274*, 23875−23882.
8. Cabral, F., and Schatz, G. (1979) One- and two-dimensional electrophoretic analysis of mitochondrial membrane proteins, *Methods Enzymol. 56*, 602−613.
9. Cabral, F., and Gottesman, M. M. (1978) The determination of similarities in amino acid composition among proteins separated by two-dimensional gel electrophoresis, *Anal. Biochem. 91*, 548−556.
10. Laemmli, U. K. (1970) Cleavage of structural proteins during the assembly of the head of bacteriophage T4, *Nature (London) 227*, 680−685.
11. Towbin, H., Staehelin, T., and Gordon, J. (1979) Electrophoretic transfer of proteins from polyacrylamide gels to nitrocellulose sheets: procedure and some applications, *Proc. Natl. Acad. Sci. U.S.A. 76*, 4350−4354.
12. Minotti, A. M., Barlow, S. B., and Cabral, F. (1991) Resistance to antimitotic drugs in Chinese hamster ovary cells correlates with changes in the level of polymerized tubulin, *J. Biol. Chem. 266*, 3987−3994.
13. Ambudkar, S. V., Dey, S., Hrycyna, C. A., Ramachandra, M., Pastan, I., and Gottesman, M. M. (1999) Biochemical, cellular, and pharmacological aspects of the multidrug transporter, *Annu. Rev. Pharmacol. Toxicol. 39*, 361−398.
14. Schiff, P. B., and Horwitz, S. B. (1980) Taxol stabilizes microtubules in mouse fibroblast cells, *Proc. Natl. Acad. Sci. U.S.A. 77*, 1561−1565.
15. Sawada, T., and Cabral, F. (1989) Expression and function of β-tubulin isotypes in Chinese hamster ovary cells, *J. Biol. Chem. 264*, 3013−3020.
16. Lopata, M. A., and Cleveland, D. W. (1987) In vivo microtubules are copolymers of available β-tubulin isotypes: localization of each of six vertebrate β-tubulin isotypes using polyclonal antibodies elicited by synthetic peptide antigens, *J. Cell Biol. 105*, 1707−1720.
17. Ahmad, S., Singh, B., and Gupta, R. S. (1991) Nucleotide sequences of three different isoforms of β-tubulin cDNA from Chinese hamster ovary cells, *Biochim. Biophys. Acta 1090*, 252−254.
18. Cabral, F., Brady, R. C., and Schibler, M. J. (1986) A mechanism of cellular resistance to drugs that interfere with microtubule assembly, *Ann. N.Y. Acad. Sci. 466*, 745−756.
19. Cabral, F., and Barlow, S. B. (1989) Mechanisms by which mammalian cells acquire resistance to drugs that affect microtubule assembly, *FASEB J. 3*, 1593−1599.
20. Gonzalez-Garay, M. L., and Cabral, F. (1995) Overexpression of an epitope-tagged β-tubulin in Chinese hamster ovary cells causes an increase in endogenous α-tubulin synthesis, *Cell Motil. Cytoskeleton 31*, 259−272.
21. Hari, M., Yang, H., Zeng, C., Canizales, M., and Cabral, F. (2003) Expression of class III β-tubulin reduces microtubule assembly and confers resistance to paclitaxel, *Cell Motil. Cytoskeleton 56*, 45−56.
22. Cabral, F., and Barlow, S. B. (1991) Resistance to antimitotic agents as genetic probes of microtubule structure and function, *Pharmac. Ther. 52*, 159−171.
23. He, L., Yang, C. H., and Horwitz, S. B. (2001) Mutations in β-tubulin map to domains involved in regulation of microtubule stability in epothilone-resistant cell lines, *Mol. Cancer Ther. 1*, 3−10.
24. Lowe, J., Li, H., Downing, K. H., and Nogales, E. (2001) Refined structure of α,β-tubulin at 3.5 Å resolution, *J. Mol. Biol. 313*, 1045−1057.
25. Li, H., DeRosier, D. J., Nicholson, W. V., Nogales, E., and Downing, K. H. (2002) Microtubule structure at 8 Å resolution, *Structure 10*, 1317−1328.
26. Cabral, F. (2000) Factors determining cellular mechanisms of resistance to antimitotic drugs, *Drug Resistance Updates 3*, 1−6.
27. Chaudhuri, A. R., Seetharamalu, P., Schwarz, P. M., Hausheer, F. H., and Luduena, R. F. (2000) The interaction of the B-ring of colchicine with α-tubulin: a novel footprinting approach, *J. Mol. Biol. 303*, 679−692.
28. Bai, R., Covell, D. G., Pei, X.-F., Ewell, J. B., Nguyen, N. Y., Brossi, A., and Hamel, E. (2000) Mapping the binding site of colchicinoids on β-tubulin, *J. Biol. Chem. 275*, 40443−40452.
29. Jung, M. K., May, G. S., and Oakley, B. R. (1998) Mitosis in wild-type and β-tubulin mutant strains of *Aspergillus nidulans*, *Fungal Genet. Biol. 24*, 146−160.
30. Bryan, J. (1972) Definition of three classes of binding sites in isolated microtubule crystals, *Biochemistry 11*, 2611−2616.
31. Ravelli, R. B. G., Gigant, B., Curmi, P. A., Jourdain, I., Lachkar, S., Sobel, A., and Knossow, M. (2004) Insight into tubulin regulation from a complex with colchicine and a stathmin-like domain, *Nature 428*, 198−202.
32. Abraham, I., Marcus, M., Cabral, F., and Gottesman, M. M. (1983) Mutations in α- and β-tubulin affect spindle formation in Chinese hamster ovary cells, *J. Cell Biol. 97*, 1055−1061.
33. Prakash, V., and Timasheff, S. N. (1992) Aging of tubulin at neutral pH: stabilization by colchicine and its analogues, *Arch. Biochem. Biophys. 295*, 146−152.

BI049637B